

RPC simulations from a current stand point

Diego Gonzalez-Diaz^{*†}

Department of Engineering Physics, Tsinghua University, Key Laboratory of Particle & Radiation Imaging, Ministry of Education, Beijing 100084, China

GSI Helmholtz Center for Heavy Ion Research, Darmstadt, Germany

Laboratorio de Física Nuclear y Altas Energías, Universidad de Zaragoza, Zaragoza, Spain

E-mail: diegogon@unizar.es

Huangshan Chen, Yi Wang

Department of Engineering Physics, Tsinghua University, Key Laboratory of Particle & Radiation Imaging, Ministry of Education, Beijing 100084, China

We scrutinize, in the simplest case (1 conductor + return), the currents induced at the readout points of various parallel plate geometries under the movement of charges as the ones created inside timing RPCs at typical operating conditions. In particular, we focus on the transition from a purely circuital description to a transmission-line one, the driving parameter being the system electrical length. Implications for the simulations of Resistive Plate Chambers within an ‘induction + transmission’ framework are discussed.

XI workshop on Resistive Plate Chambers and Related Detectors - RPC2012,

February 5-10, 2012

INFN Laboratori Nazionali di Frascati Italy

^{*}Speaker.

[†]This work is supported by the National Science Foundation of China, under grant 111050110573.

1. Introduction

Till recently, detailed Monte Carlo simulations of Resistive Plate Chambers down to charge distributions, efficiency and time resolution, have been performed by working out the induction characteristics of the stochastically growing avalanches over -just- one of the surrounding electrodes; the induction process was then modeled through an ideal current generator (obtained for instance by weighting-field techniques) that was usually sent to a bandwidth-limited amplifier-chain and finally discriminated, [1]-[5]. Authors model the readout chain in substantially different ways, however simulations share two significant facts: i) the influence of the detector capacitance and/or its characteristic impedance is often acknowledged, but never explicitly included in calculations and ii) irrespective of the bandwidth/peaking time considered, if any, the electronics threshold is characterized by an universal/shape-independent ‘threshold charge’ Q_{th} , that is either left to the experimentalist for proper determination ([6], for instance) or adjusted to describe the efficiency data. As shown later, although this great conceptual simplification (hereafter, the ‘ Q_{th} -approach’) has allowed to obtain useful simulation results, it inherently hides a difficulty with treating signal induction, transmission and read-out consistently and thus partially undermines the ability of obtaining a precise description of some of the detector characteristics, especially those concerning efficiency and timing performances, crosstalk and transmission losses in electrically-long counters, phenomena for which the signal shape at threshold is generally of greater relevance than its charge.

The success of the ‘ Q_{th} -approach’ can be understood, at least partly, in the context of readout chains that are slow compared to i) the time evolution of the electron component of the avalanches created inside the amplification gap and to ii) the typical transient times of the associated electromagnetic perturbation (ΔT) inside the whole system. Under these conditions, the observable signal amplitude is strongly related to the integral of the current induced over the pick-up electrode, with independency from its original shape, the detector capacitance and other system details. From the point of view of signal sensitivity, in particular, (i.e., efficiency), the ‘ Q_{th} -approach’ requires therefore:

1. $BW \ll f_c$,

i.e. small bandwidths of the read-out chain BW , compared to the signal cutoff frequency, f_c , as estimated from its rise-time, [7].

2. $BW^* \ll 1/\Delta T$,

where BW^* is the system bandwidth (including both signal and electronics), as estimated from the signal rise-time. In the context of transmission line theory, this condition can be written as a function of the system electrical length, Λ_e , as $\Lambda_e \ll 1$, meaning the system is electrically short. Here $\Lambda_e = BW^* \Delta T$ and $\Delta T = D/v$, where D is a characteristic propagation scale (hereafter, the length of the read-out strip) and v is the signal propagation velocity along the read-out structure.

In the context of time resolution there is yet a third condition, but this is not given here since a short discussion is neither possible nor pertinent. Thus, in other words, under conditions 1,2 the signal formation inside the readout structure can be considered to be of the δ -impulse type.

Whenever Q_{th} was experimentally determined, it has to be expected that it was also obtained under these conditions.

Since technological scenarios simultaneously dealing with $BW \sim f_c$ and $\Lambda_e = 20-40$ are nowadays either built or foreseen, [7], it is clear that a strong necessity exists to consistently develop a more general formulation of the problem of signal induction, transmission and read-out in RPCs. A first step towards avoiding the aforementioned limitations was undertaken in [8], where direct information from the signal waveforms was included in simulations in order to describe the most characteristic multi-strip observables like charge sharing and specially cross-talk, as observed in early implementations of timing RPCs with multi-strip readout.¹ The formulation, based on the ‘induction+transmission’ model, was discussed in some detail in [7]. Under this model, the fundamental quantities necessary throughout the complete detector simulation are the induced currents and no critical approximation is needed.

2. The induction+transmission model

Experimental agreement with transmission line theory has been reported for multi-strip Bakelite-based RPCs up to 0.2GHz and up to 3GHz for glass-based RPCs, under conditions of external excitation [9], [7]. On the other hand, a general framework for including any arbitrary readout network was introduced by W. Riegler in [10]. Under this perspective, one might consider the induction+transmission model proposed in [7, 8] to be an appropriate formalism for estimating the measured currents in RPCs. The formalism suggests to separate the problem in 4 steps: i) calculate the avalanche space-time charge density, ii) calculate the induced currents at a cross-section of the device by using the Shockley-Ramo theorem or its generalized version if needed [10], iii) introduce them as ideal current generators at the given longitudinal position and solve the transmission-line equations for an arbitrary load \hat{z}_0 , iv) include the readout electronics as a convolution at a later stage by identifying its input impedance with the corresponding elements of matrix \hat{z}_0 .

This procedure is very elegant, however steps ii)-iii) lack internal consistency. The reason is that derivations for generalized Shockley-Ramo theorems based on the Green’s reciprocity theorem [10], as proposed for step ii), assume there is no position dependence of the induced currents or potentials on the electrodes of interest, i.e., the system is electrically short. The latter is, however, an assumption one wants to avoid when adopting a transmission line description, as in step iii).

Theoretical caveats aside, an early implementation of the rough induction+transmission model has shown some virtues in capturing essential details of electrically-long glass-based RPCs: very high cross-talk levels under certain circumstances, lack of strong signal shaping during transmission and the relevance of the impedance mismatch on the measured efficiencies [8, 11]. Therefore, to the extent that the ‘induction+transmission’ model also recovers the exact circuitual solutions as expected from [10] when the system becomes electrically-short, another brick of evidence is added to the phenomenological relevance of such an intuitive and computationally-inexpensive model.

¹Unfortunately, the available characterization of the electronics, based on the experimental parameter Q_{th} , enforced a mixed-simulation: ‘signal shape’-dependent parameters (like the fraction of signal transmitted and cross-talk) were combined ‘ad hoc’ with a Q_{th} -based parameterization of the electronics.

We aim at illustrating this for a simple ‘1-conductor + return’ scenario, as of Fig. 1-left, within this short communication.

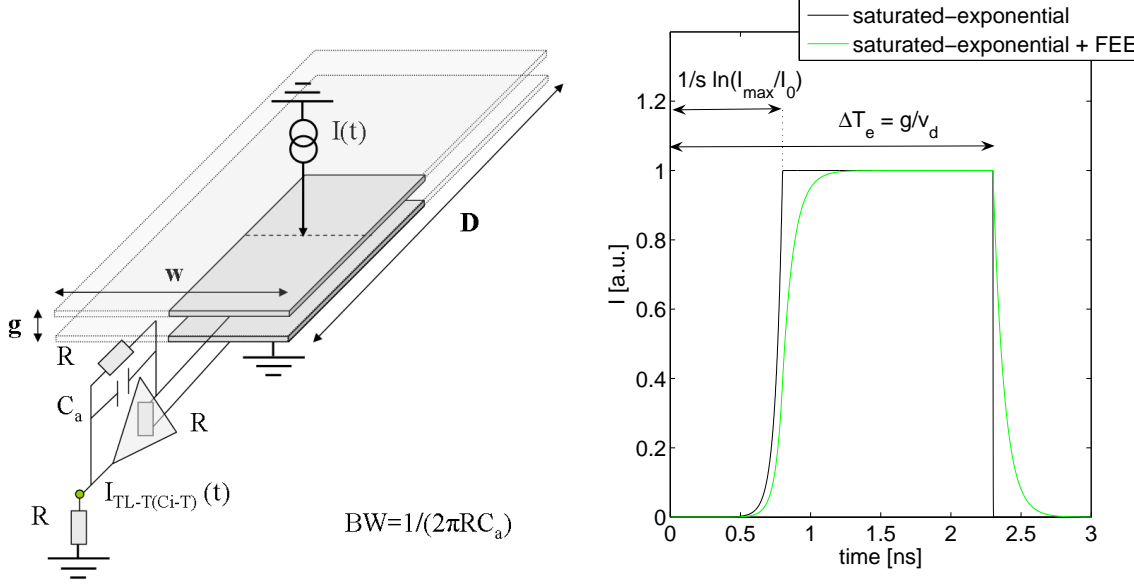


Figure 1: Left: artistic representation of the family of parallel plate geometries studied in this work. Right: a typical exponential signal at a field of 100kV/cm generated at the RPC cathode and abruptly saturating after an amplification of around $I_{max}/I_0 = 10^7$.

3. Circuit theory vs Transmission Line theory

According to the ‘induction+transmission’ framework, but also to the exact recipe given in [10] for electrically-short structures, the currents induced on the pickup electrodes $I(t)$, as a result of the charges moving in the gas gap ($q(t)$, drift velocity $v_d(t)$), have to be calculated in a first step. We assume that such a calculation can be performed in the same way within both frameworks, so it is immaterial for the forthcoming discussion. Thus, once a certain initial current $I(t)$ has been calculated, the current at the readout point (green circle in Fig. 1-left) will be obtained here under two different formalisms: a) circuit theory (subscript $Ci - T$), according to [10], and b) transmission line theory (subscript $TL - T$), according to the model under investigation, i.e., the ‘induction-transmission’ model. The general expression for the currents that are read out in a multi-conductor system across resistances R , situated just at one of the conductors ends (the other one being simply open), when the structure is excited along line -n-, are:

$$\vec{I}_{Ci-T}(t) = \frac{1}{\sqrt{2\pi}} \int_{-\infty}^{+\infty} (1 + \hat{z}^{-1}(\omega) \hat{z}_0)^{-1} \vec{I}(\omega) e^{i\omega t} d\omega \quad (3.1)$$

$$\vec{I}_{TL-T}(t) = \frac{\hat{z}_0}{R} (\hat{z}_0 + \hat{Z}_c)^{-1} \sum_{j=0}^{\infty} ((\hat{z}_0 - \hat{Z}_c)(\hat{z}_0 + \hat{Z}_c)^{-1})^j \hat{Z}_c \hat{M} \begin{pmatrix} \hat{M}_{1n}^{-1} \{ I(t - \frac{y_0 + 2jD}{v_1}) + I(t - \frac{2(j+1)D - y_0}{v_1}) \} \\ \dots \\ \hat{M}_{Nn}^{-1} \{ I(t - \frac{y_0 + 2jD}{v_N}) + I(t - \frac{2(j+1)D - y_0}{v_N}) \} \end{pmatrix} \quad (3.2)$$

where we have assumed at this point that $C_a \rightarrow 0$ (infinite bandwidth) and:

$$\vec{I}(\omega) = \frac{1}{\sqrt{2\pi}} \int_{-\infty}^{+\infty} \vec{I}(t) e^{-i\omega t} dt \quad (3.3)$$

Following the notation in [7], matrixes are represented by $\hat{\cdot}$, while $\vec{I}(t) = \{0, \dots, 0_{n-1}, I(t), 0_{n+1}, \dots, 0_N\}$ is the vector of initial currents and $\vec{I}(\omega)$ its Fourier Transform. Besides magnitudes connected to the numerical solutions of the transmission line equations (matrix of eigenvectors \hat{M} , eigenvalues v_{1-N}), it is important to note in eqs. 3.1, 3.2 the presence of both the RPC electrical and characteristic impedance matrixes (\hat{z} , \hat{Z}_c , respectively), as well as the impedance matrix of the read-out network \hat{z}_0 . Eq. 3.1 can be simply deduced by applying the terminal conditions and the generalized Norton theorem ([14], for instance) while eq.3.2 is a particular case of eq. (10) in [7].

Unlike \hat{z} , the characteristic impedance \hat{Z}_c can be regarded as frequency-independent for most practical purposes, except if losses are important (see [7]). Yet, in the typical case where losses with respect to the return conductor (dielectric) or along the driven one (resistive) are dominant over the effect of other conductors, a convenient factorization is possible, resulting in:

$$\vec{I}_{TL-T}(t) = \frac{1}{\sqrt{2\pi}} \int_{-\infty}^{+\infty} \vec{I}_{TL-T}(\omega) e^{-D/\Lambda(\omega)} e^{i\omega t} d\omega \quad (3.4)$$

where $1/\Lambda(\omega)$ is the attenuation constant [7]. When aiming at a circuital description, losses, if present, are included through $\hat{z}(\omega)$.

Finally, the electronics response function $h(t)$, can be included in a last step as:

$$\vec{I}_{TL-T}''(t) = \frac{1}{\sqrt{2\pi}} \int_{-\infty}^{+\infty} \vec{I}_{TL-T}(\omega) h(\omega) e^{i\omega t} d\omega \quad (3.5)$$

as well as:

$$\vec{I}_{CT-T}(t) = \frac{1}{\sqrt{2\pi}} \int_{-\infty}^{+\infty} \vec{I}_{CT-T}(\omega) h(\omega) e^{i\omega t} d\omega \quad (3.6)$$

that would equal:

$$h(\omega) = \frac{1}{1 + RC_a \omega j} \quad (3.7)$$

for the simple case discussed in Fig. 1-left.

For practical RPCs, the general solution to the Transmission Line problem including losses and electronics might be thus obtained via eqs. 3.2, 3.4, 3.5. If the system has a double-end readout, eq. 3.2 has to be replaced by eq. (10) in [7]. The validity of this approach was verified experimentally in [7] for the case of external excitation.

It is daring to say that eqs. 3.1 and 3.2 may coincide in some limit, however this is -exactly- what happens in the limit $BW \rightarrow 0$ (that fulfills in practice the two conditions required by the ‘ Q_{th} -approach’). Proving such a limit can be routinely done with any commercial circuit solver. In the following, we perform equivalent simulations for the structure of Fig. 1 by using custom-developed OCTAVE/MATLAB routines. Only the ‘1 conductor + return’ scenario will be discussed here so all vectors and matrixes in eqs. 3.1, 3.2 collapse to scalars.

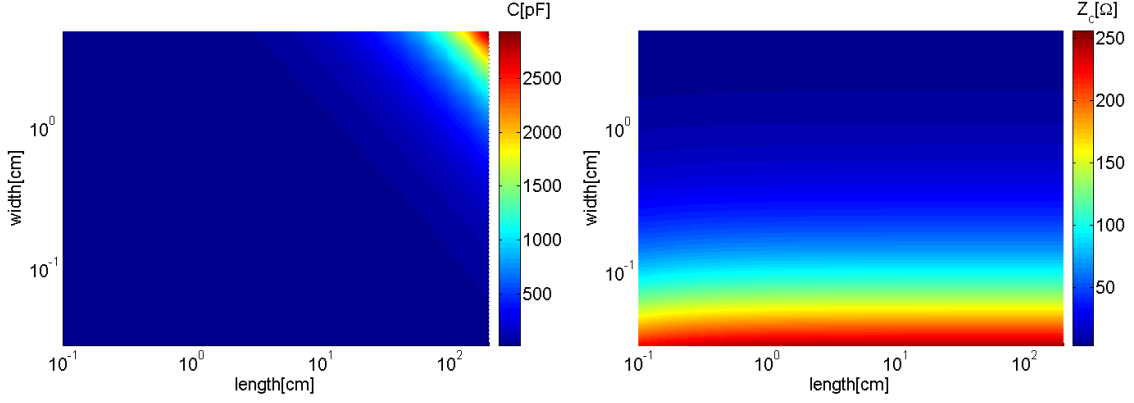


Figure 2: Left: calculated capacitances as a function of the width and length of the structure shown in Fig.1-left, under approximation [12]. Right: the associated characteristic impedance.

4. Results for parallel plate structures with 1 conductor + return

We chose a characteristic avalanche signal as created by a free electron originated at the cathode, assuming space-charge suddenly stops the growth at a signal multiplication of roughly $I_{max}/I_0 \simeq 10^7$, [8]. Further parameters are $v_d = 0.02\text{cm/ns}$ and $\alpha - \eta = 100\text{mm}^{-1}$, as obtained at a field of 100kV/cm for pure $\text{C}_2\text{H}_2\text{F}_4$, [13], and extrapolated to $P = 1\text{atm}$, $T = 20^\circ\text{C}$. The resulting signal, arbitrarily normalized to 1 at maximum is given in Fig. 1-right (in black):

$$I(t) = e^{S(t-t_{max})}\Theta(t)\Theta(t_{max}-t) + \Theta(t-t_{max})\Theta(\Delta T_e-t) \quad (4.1)$$

where $S = (\alpha - \eta)v_d$, the time at maximum is $t_{max} = \frac{1}{S} \ln I_{max}/I_0$ and the avalanche transient time is $\Delta T_e = g/v_d$, with g the gas gap. We include, for realism, a bandwidth-limited electronics implemented as a low-pass circuit, with $BW = 2\text{GHz}$ (Fig. 1-right (green)). It is clear that for multiple avalanches, in first order, the resulting induced signals can be considered to be a superposition of such type of elementary signals (see 1D-models in [2, 3] as well as [8]).

For this exercise, we purposely avoid usage of any commercial software and take as electrostatic parameters the 1D parameterization given by Xiang, in [12], for the capacitance of a parallel plate geometry including fringe fields. We extend it to 2D by assuming fringe fields on each plate side to be independent, so that:

$$C = \epsilon_0 \frac{WD}{g} + DC_{f,w}(W/g) + WC_{f,D}(D/g) \quad (4.2)$$

Here C_f are the fringing capacitances as given in [12]. In this particular case:

$$Z_c = \frac{D}{vC} \quad (4.3)$$

$$z = \frac{1}{j\omega C} \quad (4.4)$$

where v equals the speed of light, c . The outcome of this parameterization is shown in Fig. 2.

We let W and D vary logarithmically on intervals $[0.03, 5]\text{cm}$, for the former, and $[0.1, 200]\text{cm}$, for the latter. The upper bound of W is chosen such that the system is electrically short across its

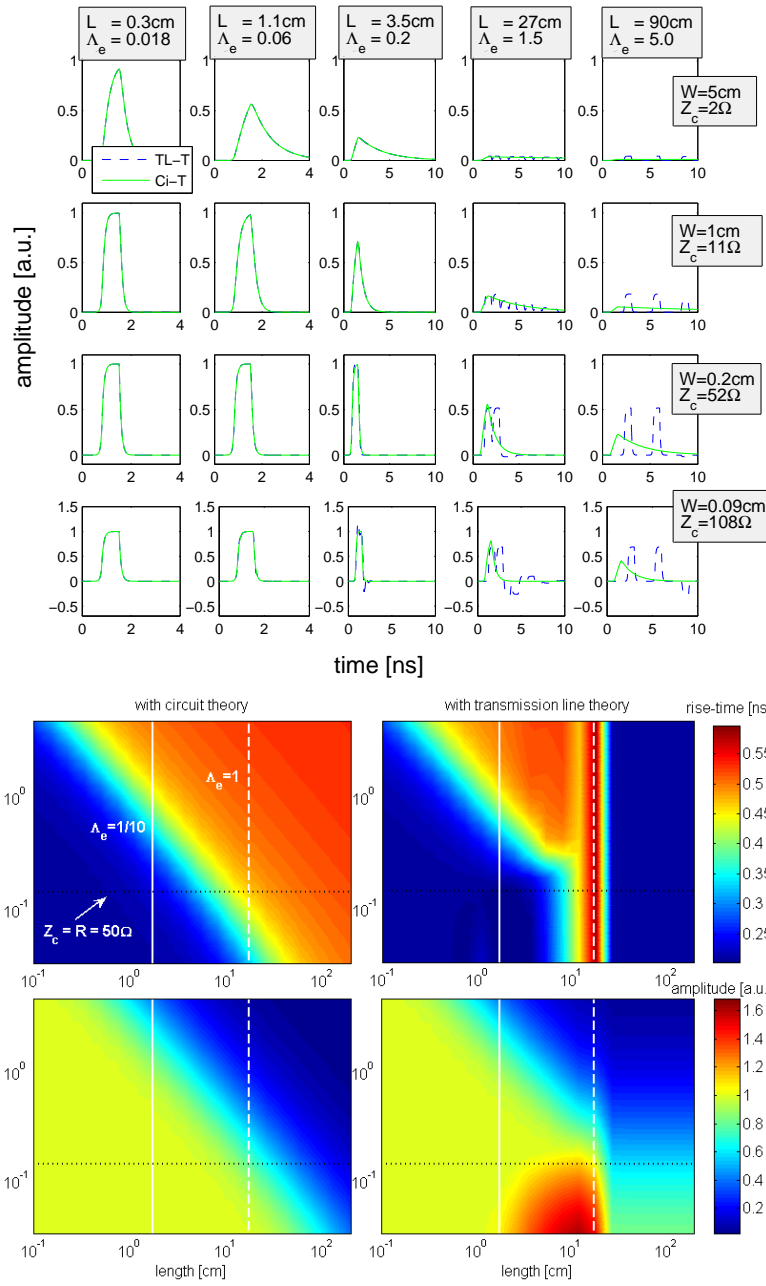


Figure 3: Up: waveforms for several structures under circuit theory (Ci-T) and transmission line theory (TL-T). Discrepancies appear around $\Lambda_e = 1$, and become more pronounced for higher characteristic impedances. Down: 2-dimensional representation of the main signal parameters (rise-time and amplitude) under a circuitual description and a transmission-line one.

dimensions. Violating such a condition invalidates both circuit theory and transmission line theory at once, [14], and lays therefore beyond the scope of this discussion. A selection of waveforms is given in Fig. 3-up. The electrical length $\Lambda_e = BW^*D/c$ relates to the system bandwidth BW^* , that is well approximated by the cutoff frequency of the exponential rise-time component $f_c = S/2\pi$ in

quadrature with the amplifier bandwidth, hence:

$$\frac{1}{BW^{*2}} = \frac{1}{f_c^2} + \frac{1}{BW^2} \quad (4.5)$$

If a dielectric media different from vacuum is present, the electrical length is reduced in inverse proportionally to its dielectric constant $\sqrt{\epsilon_r}$.

By observing Fig. 3-up, it can be seen that deviations from circuit theory become important around $\Lambda_e = 1$, as expected. The agreement below $\Lambda_e = 1$ is remarkable, however the amount of reflections necessary for a good description based on eq. 3.2 can reach 100, so that a simple convolution might be faster in such a case and a circuital solution preferable. Note that the regime where a transmission line description is favored over a circuital one, broadly speaking, is situated in the range $\Lambda_e > [\frac{1}{10}, 1]$, [14]. However this criteria, as indicated by the upper and lower bounds inside the brackets is, in detail, pretty much system-dependent. This fact can be observed, for instance, through a more detailed comparison performed on the basis of 2D representations of the main parameters of the signal: its rise-time (defined from 10%-90%) and amplitude (Fig. 3-down). The conclusion is similar, in the regime $\Lambda_e < 1$ circuit theory offers an increasingly good approximation, however an accurate description requires using transmission line theory from $\Lambda_e > 1/10$ on. It is interesting to note the region around $\Lambda_e \sim 1$, where the discrepancies in the signal rise-times are very high. This is due to the constructive interference between the direct and reflected waves. This effect is expected, however its practical importance in timing depends critically on the threshold levels since, whenever shaping is present, the signal rise-time can be easily much larger than the one obtained from the relative slope $(\ln 9(1/IdI/dt)^{-1})$ at fixed threshold. With a double-end readout the effect is further minimized since reflections are suppressed due to the relatively small FEE input impedance, while in the present case reflections have the same amplitude than the direct signal. This particular feature of the single-end readout was very much emphasized by the HARP collaboration ([15] and references therein).

5. Discussion

We have presented a systematic comparison between transmission line theory and circuit theory for several parallel plate geometries. This (intentionally) simplified study, in connection to previous results [7, 8] aims at illustrating the power of the ‘induction + transmission’ model, that includes transmission line theory as one of the intermediate steps. We have verified that the role of the characteristic impedance Z_c in a transmission-line description consistently replaces the role of the electrical impedance (through its capacitance C) in the limit where the system becomes electrically-short. Thus, the former scenario simply offers a more general way to perform calculations.

Further insight can be obtained by studying the rise-time and signal amplitude of the simulated signals as a function of the RPC length, as done in Fig. 4. The circuit-theory approximation shows a smooth behavior and, indeed, a very accurate approximation to the signal amplitude can be obtained analytically as:

$$I_{max} = 1 - e^{-\frac{\Delta T_e}{RC(D,W)}} \quad (5.1)$$

A reasonable approximation to the signal rise-time (although not exact) is:

$$t_{rise} = \frac{\ln 9}{2\pi} \sqrt{\frac{1}{f_c^2} + \frac{1}{BW^2} + (2\pi RC(D, W))^2}$$

$$t_{rise} = \frac{\ln 9}{2\pi BW^*} \sqrt{1 + (2\pi BW^* RC(D, W))^2} \quad (5.2)$$

It is interesting to note that the signal amplitude is connected to the ratio between the signal width and the RC defined between the readout resistance and the RPC capacitance. The rise-time is, however, mainly connected to the product of the system bandwidth BW^* , defined from eq. 4.5, and the RC.

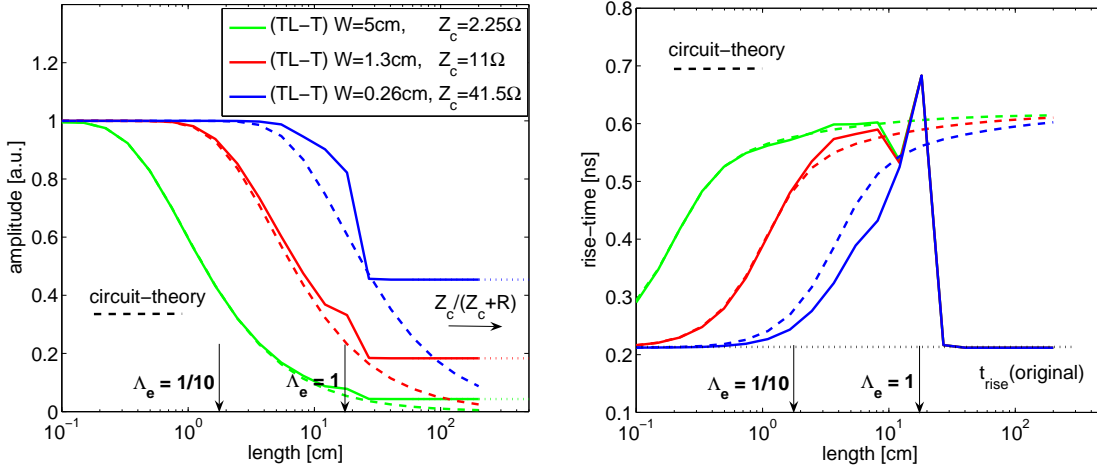


Figure 4: Left: comparison of the RPC signal amplitude observed at the readout point as a function of the length of the parallel plate structure on which it has been induced. Simulations for both circuit-theory (dashed lines) and transmission line theory (continuous line, label TL-T). Right: similar systematics, but for the signal rise-time.

An important consequence of the transmission+induction model is that, from the point of view of the signal rise-time, the larger the transmission, the better, except if losses (through the attenuation coefficient $1/\Lambda(\omega)$) are important (they have been neglected here). Moreover, if the system is matched ($Z_c = R$) at both ends, there will be absence of shaping with independence from the detector length. This result is widely known for transmission lines excited from one end, but how to reconcile this apparently universal absence of shaping with the case of internally excited systems that are perfectly matched and describable with circuit theory, where shaping is expectedly governed by RC ? For that, one should recall eq. 4.3 under the condition $Z_c = R$. We then obtain for a matched strip, in the circuit theory limit ($\Lambda_e \ll 1$), the condition:

$$BW^* RC \ll 1 \quad (5.3)$$

implying that the RPC capacitance C and the readout resistance R do not contribute substantially to the signal shape (characterized by BW^*). This ensures, therefore, consistency with a transmission-line formulation also in the case of matched systems.

6. Conclusion

We have shown consistency between a circuital description and a slightly more general, yet computationally affordable, ‘induction+transmission’ model in some particular cases of interest for RPC simulations. Given the fact that such a model has previously shown potential to describe performances of electrically-long multi-conductor (i.e. multi-strip) RPCs, we believe it has a great phenomenological power for extending RPC simulations beyond the old single-cell scenario.

References

- [1] E. Cerron Zeballos et al., *Avalanche fluctuations within the multigap resistive plate chamber*, Nucl. Instr. Meth. A, 381(1996)569.
- [2] M. Abbrescia et al., *Resistive Plate Chambers in avalanche mode: a comparison between model predictions and experimental results*, Nucl. Instr. Meth. A, 409(1998)1.
- [3] M. Abbrescia et al., *Progresses in the simulation of resistive plate chambers in avalanche mode*, Nucl. Phys. B (Proc. Suppl.), 78(1999)459.
- [4] W. Riegler, C. Lippmann, R. Veenhof, *Detector physics and simulation of resistive plate chambers*, Nucl. Instr. Meth. A, 500(2003)144.
- [5] C. Lippmann and W. Riegler, *Space charge effects in Resistive Plate Chambers*, Nucl. Instr. Meth. A, 517(2004)54 and references therein.
- [6] P. Fonte et al., *High resolution RPCs for large TOF systems*, Nucl. Instr. Meth. A, 449(2000)295.
- [7] Diego Gonzalez-Diaz, Huangshan Chen, Yi Wang, *Signal coupling and signal integrity in multi-strip resistive plate chambers used for timing applications*, Nucl. Instr. Meth. A, 648(2011)52.
- [8] D. Gonzalez-Diaz, *Simulation of resistive plate chambers with multi-strip readout*, Nucl. Instr. Meth. A, 661(2012)172.
- [9] Werner Riegler and Daniel Burgarth, *Signal propagation, termination, crosstalk and losses in resistive plate chambers* Nucl. Instr. Meth. A, 481, 1-3(2002)130.
- [10] W. Riegler, *Expanded theorems for signal induction in particle detectors*, Nucl. Instr. Meth. A, 535(2004)287.
- [11] I. Deppner, N. Herrmann, D. Gonzalez-Diaz et al., *The CBM time-of-flight wall*, Nucl. Instr. Meth. A, 661(2011)121.
- [12] Y. Xiang, *The electrostatic capacitance of an inclined plate capacitor*, J. Electrostatics, 64(2006)29.
- [13] J. de Urquijo et al., *Electron swarm coefficients in 1,1,1,2 tetrafluoroethane (R134a) and its mixtures with Ar*, Eur. Phys. J. D, 51(2009)241.
- [14] C. R. Paul, *Analysis of Multiconductor Transmission Lines*, John Wiley & Sons, 2008.
- [15] V. Ammosov et al., *The HARP resistive plate chambers: Characteristics and physics performance*, Nucl. Instr. Meth. A, 578(2007)119.